

Constraints on single-field inflation with WMAP, SPT and ACT data— A last-minute stand before Planck

Cheng Cheng^{1,2 *}, Qing-Guo Huang^{1 †}, Yin-Zhe Ma^{3,4 ‡}

¹ State Key Laboratory of Theoretical Physics, Institute of Theoretical Physics, Chinese Academy of Sciences, Beijing 100190, China

² University of the Chinese Academy of Sciences, Beijing 100190, China

³ Department of Physics and Astronomy, University of British Columbia, Vancouver, V6T 1Z1, BC Canada

⁴ Canadian Institute for Theoretical Astrophysics, 60 St. George Street Toronto, M5S 3H8, Ontario, Canada

ABSTRACT: We constrain models of single field inflation with the pre-*Planck* CMB data. The data used here is the 9-year Wilkinson Microwave Anisotropy Probe (*WMAP*) data, South Pole Telescope (SPT) data and Atacama Cosmology Telescope (ACT) data. By adding in running of spectral index parameter, we find that the χ^2 is improved by a factor of $\Delta\chi^2 = 8.44$, which strongly indicates the preference of this parameter from current data. In addition, we find that the running of spectral index α_s does not change very much even if we switch to different pivot scales, which suggests that the power law expansion of power spectrum is accurate enough till the 1st order term. Furthermore, we find that the joint constraints on $r - n_s$ give very tight constraints on single-field inflation models, and the models with power law potential ϕ^p can only survive if $0.9 \lesssim p \lesssim 2.1$, so a large class of inflation models have already been ruled out before *Planck* data. Finally, we use the f_{NL} data to constrain the non-trivial sound speed c_s . We find that the current constraint is dominated by the power spectrum constraints which have some inconsistency with the constraints from f_{NL} . This poses important questions of consistency between power spectrum and bispectrum of *WMAP* data.

KEYWORDS: CMB, inflation.

*chcheng@itp.ac.cn

†huangqg@itp.ac.cn

‡mayinzhe@phas.ubc.ca

Contents

1. Introduction	1
2. Methodology	2
2.1 The Model	2
2.2 The data	4
3. Results	4
3.1 Canonical single-field slow-roll inflation model ($c_s = 1$)	4
3.1.1 Λ CDM cosmology model	4
3.1.2 Comparison of different pivot scale and the influence of running of runing of spectral index (β_s)	8
3.2 General single-field inflation Model (c_s free)	10
4. Conclusion	10

1. Introduction

The inflationary model [1, 2, 3] has achieved a great success in modern cosmology, and it has been confirmed by many high precision CMB and Large scale structure experiments [4, 5, 6]. It provides a good explanation to a series problems such as flatness problem, horizon problem, and monopole problem in the standard cosmology scenario. In addition, inflation paradigm provides a natural explanation for the origin of primordial perturbations which constitute the seeds for the large scale structure we can see today. Therefore, identifying the realistic inflation model becomes an important task in observational cosmology.

Astronomical observations provide a large mount of data to constrain the cosmological parameters, especially inflation models. The default cosmology model people always use is the “six-parameter” Λ CDM cosmology model, in which the canonical single-field slow-roll inflation (sound speed $c_s = 1$) is assumed in the model. However, the class of slow-roll inflation models already have some weak tension with the observational data. In Ref. [4], it is shown that the generic ϕ^p inflation model cannot provide consistent $r - n_s$ values within reasonable range of number of e -folds. In addition, *WMAP* 9-year data [7] suggests that the local non-Gaussianity has a large positive value, while the orthogonal non-Gaussianity is a large negative value, and these values are hardly to be produced in the canonical single-field slow-roll inflation models. Given these interesting tension between the canonical single-field slow-roll inflation model and the current observational data, we would like to explore the possibilities of non-trivial sound speed $c_s \neq 1$ as well as non-zero running of spectral index $dn_s/d\ln k$ to test their consistency with current combination of *WMAP* 9-year data [4],

ACT data [6] and SPT data [5]. We intend to finish this work right before *Planck* data release (expected on 21st March, 2013) in order to make an immediate comparison before and after the *Planck* data. We hope that our work will motivate theorists to explore more phenomena in the general single-field slow-roll inflation model given the tight constraints on single field inflation models.

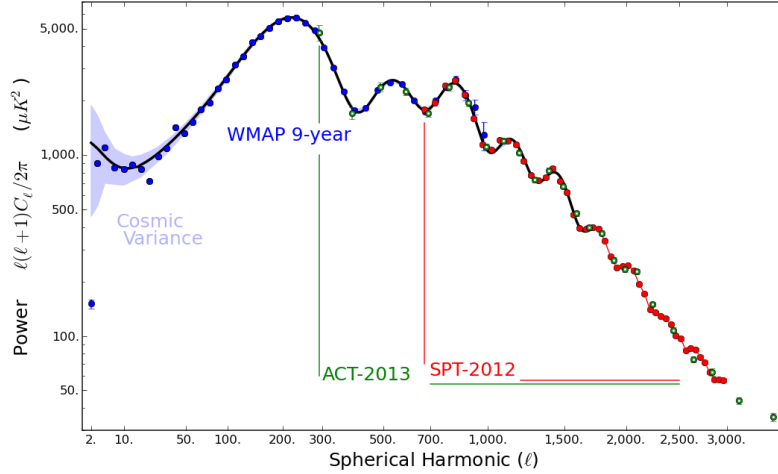


Figure 1: *WMAP*9 temperature data with lensed ACT and SPT data. *WMAP*9, ACT and SPT data are mainly in the range $2 \leq l \lesssim 1000$, $300 \lesssim l \lesssim 3000$, and $700 \lesssim l \lesssim 3000$ respectively. The theoretical curve is the lensed CMB power spectrum with *WMAP* 9-year cosmological parameters and the light blue band is the cosmic variance. The *Planck* data will further tighten up the error-bars in the middle regime. This figure is reprinted with permission from Mark Halpern.

This paper is organized as follows. In Sec. 2, we will discuss the model we are focusing on, and the data we will use to constrain the models. In Sec. 3, we will present our results of fitting. The concluding remarks will be presented in the last section.

2. Methodology

2.1 The Model

We will use standard 6-parameter Λ CDM model as our basic model¹. We then allow r (tensor-to-scalar ratio), $dn_s/d\ln k$ (running of spectral index), c_s (sound speed for the curvature perturbation modes) to be varied since we want to explore the level of constraints from these parameters. The sound speed is related to the tilt of tensor power spectrum in

¹The free running parameters are $\{\Omega_b h^2, \Omega_c h^2, \Omega_\Lambda, \tau, n_s, A_s\}$, which are fractional baryon, cold dark matter, and dark energy density, optical depth, spectral index and amplitude of primordial scalar perturbation respectively.

the general single-field inflation model through [8, 9]²

$$n_t = -\frac{r}{8c_s}, \quad (2.1)$$

where the tensor power spectrum is parameterized as

$$P_t(k) = A_t(k_0) \left(\frac{k}{k_0} \right)^{n_t}, \quad (2.2)$$

Here k_0 is the pivot scale. Thus the tensor to scalar ratio is defined as

$$r = \frac{A_t(k_0)}{A_s(k_0)}. \quad (2.3)$$

Since tensor power spectrum also contribute to CMB angular power spectrum C_l^{TT} on very large scales, we will use the CMB temperature angular power spectrum to constrain r and c_s . For more discussion on how the sound speed c_s changes the data fitting is given in [10].

In addition, we add the “running of running” parameter which characterizes the running of running of spectral index, i.e.

$$\beta_s = \frac{d\alpha_s}{d \ln k} = \frac{d^2 n_s}{d \ln k^2}. \quad (2.4)$$

Thus the scalar power spectrum is parameterized as

$$P_s(k) = A_s(k_0) \left(\frac{k}{k_0} \right)^{n_s(k_0) - 1 + \frac{1}{2} \alpha_s(k_0) \ln \left(\frac{k}{k_0} \right) + \frac{1}{6} \beta_s \ln^2 \left(\frac{k}{k_0} \right)}. \quad (2.5)$$

Note that once the “running of running” (β_s) is introduced into the model, the running of spectral index α_s becomes a scale-dependent quantity. To remove any ambiguity, we need to specify the pivot scale in the power law expansion (Eq. (2.5)), this is why the α_s is related to k_0 . However, if α_s turns out to be less dependent on k_0 , it means that the truncation till α_s is enough (1st order), and there is no need to introduce a higher order truncation (β_s).

The reason we want to release β_s as the running of running parameter is that SPT data [5] gives a detection of a negative value of the running of spectral index $\alpha_s = dn_s/d \ln k$ at $k_0 = 0.025 \text{Mpc}^{-1}$. So we would like to add this parameter as a higher order effect to monitor any possible “running of running”. Even though it has not been detected, it is expected to be significantly constrained and is useful for the reconstruction of canonical single-field slow-roll inflation [11, 12].

²Here we assume c_s as a constant. The perturbation mode with sound speed c_s crosses horizon during inflation when $c_s k = aH$. Considering $n_s - 1 = -2\epsilon - \eta - s \sim \mathcal{O}(10^{-2})$ and both slow-roll parameters ϵ and η are far less than 1, we conclude that $s \sim \mathcal{O}(10^{-2})$, where $s \equiv \frac{c_s}{H c_s}$. On the other hand, since $d \ln k \simeq H dt$, $d \ln c_s / d \ln k = s$ and then $c_s(k) = c_s(k_0) \left(\frac{k}{k_0} \right)^s$ which shows that c_s is roughly scale independent.

2.2 The data

We will use the most precise class of CMB data up-to-date, which is the combination of *WMAP* 9-year data [4], SPT data [5] and ACT data [6]. The temperature angular power spectrum from three data sets is shown in Fig. 1. The combined data is named as “*CMB* data” in the following discussion. We set the maximum l -range of scalar model to be 7000 ($l_{max}^s = 7000$), and maximal tensor l -range to be 3000 ($l_{max}^t = 3000$) in the running of MCMC chains. In addition, we add Baryon Acoustic Oscillation data [13] as well as H_0 prior from HST (Hubble-Space-Telescope) project [14] into our data source. In order to explore the variation of sound speed, we add constrained f_{NL} data provided by *WMAP* 9-year bispectrum into our likelihood. The sound speed c_s is related to the equilateral and orthogonal type of non-Gaussianity f_{NL} through Eq.(57) in [7]. So according to [7] we assign $f_i = (f_{NL}^{eq}, f_{NL}^{orth})$ as the data vector, which is

$$f_{NL}^{eq} = 51 \pm 136 \quad (-221 < f_{NL}^{eq} < 323 \text{ at } 95\% \text{CL}), \quad (2.6)$$

$$f_{NL}^{orth} = -245 \pm 100 \quad (-445 < f_{NL}^{orth} < -45 \text{ at } 95\% \text{CL}). \quad (2.7)$$

Then we use the χ^2 function (Eq.(58) in [7]) to calculate the best-fit value of c_s ³, i.e.

$$\chi^2 = \sum_{ij} f_i F_{ij} f_j - 2 \sum_i F_{ii} f_i \hat{f}_i + \sum_{ij} \hat{f}_i F_{ii} F_{ij}^{-1} F_{jj} \hat{f}_j \quad (2.8)$$

where F_{ij} is the lower right four elements of the Fisher Matrix

$$F = \begin{pmatrix} 25.25 & 1.06 & -2.39 \\ 1.06 & 0.54 & 0.20 \\ -2.39 & 0.20 & 1.00 \end{pmatrix} \times 10^{-4}, \quad (2.9)$$

and $\hat{f}_i = (51, -245)$.

For the extended model of Λ CDM, we will release r and α_s in the CAMB code [15] and further modify the code to incorporate running of running parameter (β_s). We run CosmoMC [16, 17] to generate MCMC samples. We will express our results in term of best-fit value of marginalized likelihood, as well as 1σ and 2σ confidence level (CL) (68.3% and 95.4% CL).

3. Results

3.1 Canonical single-field slow-roll inflation model ($c_s = 1$)

3.1.1 Λ CDM cosmology model

We first fix $c_s = 1$ and investigate the constraints on parameters r and α_s . The data sets we use here are *CMB* data, *BAO* and *H0*. Here we consider “6-parameter model”, “6-parameter+ r model”, “6-parameter+ α_s ” model and “6-parameter+ $r+\alpha_s$ ” model which are expressed as “ Λ CDM”, “ Λ CDM+ r ”, “ Λ CDM+ α_s ” and “ Λ CDM+ $r+\alpha_s$ ” models respectively.

³The parameter A in Eq.(57) in [7] is running as a free parameter.

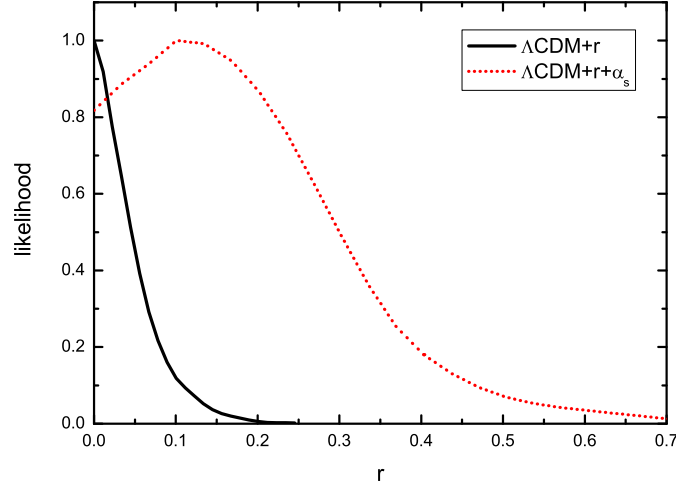


Figure 2: Likelihood of r in case of α_s fixed and α_s as free parameter.

In Fig. 2, we can see that the likelihood of r shifts a little if we switch α_s on and off. The solid line is $\Lambda\text{CDM}+r$ model, and the dotted line is $\Lambda\text{CDM}+r+\alpha_s$ model. In addition, the likelihood becomes broader in $\Lambda\text{CDM}+r+\alpha_s$ model, and the upper limit is also higher. This indicates that without the direct polarization power spectrum, it is hard to draw concrete upper limit on the amplitude of tensor mode r , since adding a single extra-parameter can greatly broaden the constraint on r .

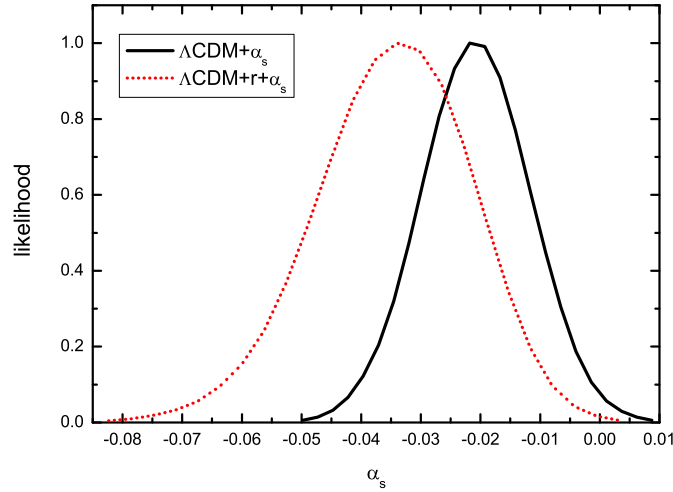


Figure 3: Likelihood of α_s in case of r fixed and r free.

Similar thing exists in Fig. 3. The solid line is the $\Lambda\text{CDM}+\alpha_s$, and the dotted one is $\Lambda\text{CDM}+\alpha_s+r$. One can see that the likelihood of α_s is broader if r is released as a free

parameter. This means that the two parameters have some level of degeneracy, which is potentially able to be broken if the future polarization data is added.

The Fig. 4 shows the likelihoods of n_s for three models. Here we consider all of the three models, i.e. $\Lambda\text{CDM}+r$, $\Lambda\text{CDM}+\alpha_s$, $\Lambda\text{CDM}+r+\alpha_s$. We can see that not only the peak of distribution shift, but also the range of confidence level of n_s changes quite a lot in three different model: if we add r , the spectral index still prefers a “red” spectrum as $n_s < 1$, but such situation does not exist anymore in the case of $\Lambda\text{CDM}+\alpha_s$ and $\Lambda\text{CDM}+\alpha_s+r$.

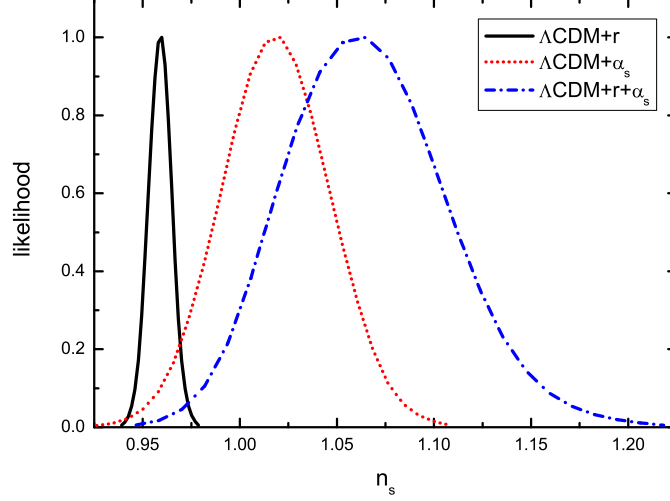


Figure 4: Likelihood of n_s in different models.

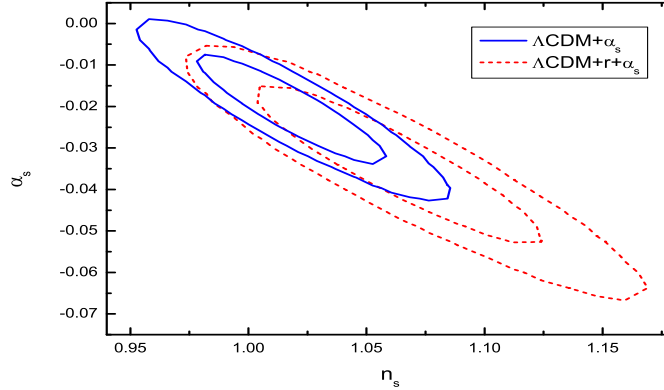


Figure 5: Joint constraint of n_s and α_s in $\Lambda\text{CDM}+\alpha_s$ (blue solid contours) and $\Lambda\text{CDM}+\alpha_s+r$ model (red dashed contours). The contours show 1σ and 2σ constraints.

Fig. 5 shows the contours of joint constraints on $\alpha_s - n_s$ in $\Lambda\text{CDM}+\alpha_s$ model (the blue solid curves) and $\Lambda\text{CDM}+r+\alpha_s$ model (the red dashed curves). We can see adding r leads to the shift of n_s towards bluer region, and the constraints become broader.

In Table 1, we list the results of fitting by fixing $c_s = 1$. One can see that by introducing α_s parameter, the χ^2 really improve significantly ($\Delta\chi^2 = 4.22$), indicating that the current data prefer the inflation model with running of the spectral index.

In the left panel of Fig. 6, we compare our joint constraints on r and n_s with the results from *WMAP* 9-year paper [4]. *WMAP* 9-year results used *WMAP* 9-year data, combined with old SPT data, old ACT data, BAO data and H_0 data and obtain the black contours (1σ and 2σ CL). We used the similar combination, except that our SPT and ACT data are the corresponding new data sets [5, 6]. By updating the new data of ACT and SPT, one can see that the constraints are tightened up to some extent. This suggests that the new SPT and ACT data really provide a large level arm for *WMAP*9 data, which offer more constraining power on small scales CMB angular power spectrum.

We use our results of joint constraints on plane of $r - n_s$ to discuss its implication for inflation models (Right panel of Fig. 6).

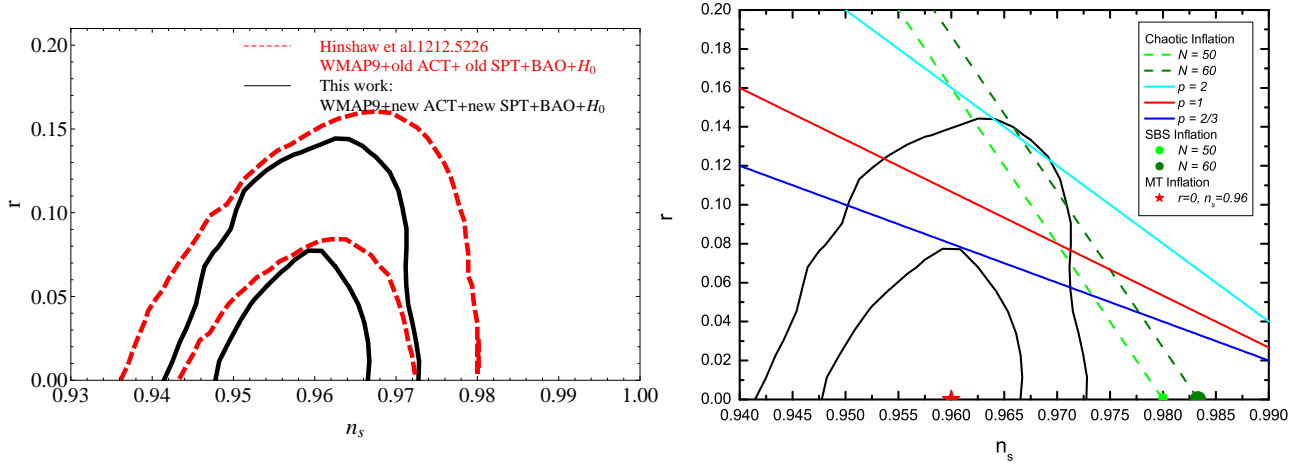


Figure 6: Joint constraint on $r - n_s$ and comparing with *WMAP*9+old SPT+old ACT (left panel) and model predictions (right panel). Left panel: the red contours are from *WMAP* 9-year results [4] which combined *WMAP*9+old ACT+old SPT+BAO+ H_0 , while our constraints are the results of *WMAP*9+new ACT+new SPT+BAO+ H_0 . Right panel: we consider several typical inflation models. (1) chaotic inflation model [18] with potential $V(\phi) \propto \phi^p$. The solid lines correspond to the predictions for different value of p , and the shallow and darker green dashed lines correspond to the predictions for $N = 50$ and $N = 60$ in the models with different power index p . (2) spontaneously broken SUSY (SBS) inflation model whose potential is given by $V(\phi) = V_0 \left(1 + c \ln \frac{\phi}{Q} \right)$ which is assumed to be dominated by V_0 . (3) mass term (MT) inflation model with potential $V(\phi) = V_0 - \frac{1}{2}m^2\phi^2$ where the mass term is assumed to be subdominant.

- Chaotic inflation model [18] whose potential is given by $V(\phi) \propto \phi^p$. This model predicts $r = \frac{4p}{N}$, $n_s = 1 - \frac{p+2}{2N}$, where N is the number of e-folds before the end of inflation. Given the current constraints on the amplitude of inflation and the “slow-roll” parameter, N is around 60 but with some uncertainty of reheating process. Here we take the range of 50-60 as the reasonable range of number of e-folds. The region

Table 1: Results of fitting by fixing $c_s = 1$. We set $k_0 = 0.002 \text{Mpc}^{-1}$, $l_{max}^s = 7000$, and $l_{max}^t = 3000$ in the running of MCMC chains.

	ΛCDM	$\Lambda\text{CDM}+r$	$\Lambda\text{CDM}+\alpha_s$	$\Lambda\text{CDM}+r+\alpha_s$	$\Lambda\text{CDM}+r+\alpha_s+\beta_s$
n_s	0.961 ± 0.007	0.959 ± 0.006	1.018 ± 0.027	1.066 ± 0.040	1.089 ± 0.080
$r(95\%CL)$	–	< 0.12	–	< 0.42	< 0.53
α_s	–	–	-0.021 ± 0.009	-0.035 ± 0.012	-0.050 ± 0.057
β_s	–	–	–	–	0.005 ± 0.021
Best fit $-\ln(\text{Like})$	4921.52	4921.15	4917.30	4916.91	4917.54
$\Delta\chi^2$	0	-0.74	-8.44	-9.22	-7.96

between two dashed lines in Fig. 6 indicates the prediction of chaotic inflation. One can see that the models with $p = 2$ [18] and $p = 2/3$ [19] are disfavored at around 2σ level, and only the models with $p \in [0.9, 1.8]$ for $N = 50$ or $p \in [1.5, 2.1]$ for $N = 60$ are still consistent with data within 95% CL.

- Spontaneously broken SUSY (**SBS**) inflation model [20] with potential $V(\phi) = V_0 \left(1 + c \ln \frac{\phi}{Q}\right)$, where the potential is assumed to be dominated by V_0 and $c \ll 1$. This model predicts $r = 0$ and $n_s = 1 - \frac{1}{N}$. The spectral index in this model is quite large and it is disfavored at more than 95% CL.
- Mass term (**MT**) inflation model [21] with potential $V(\phi) = V_0 - \frac{1}{2}m^2\phi^2$ where the mass term is assumed to be subdominant. The tensor-to-scalar ratio and spectral index in this model are respectively given by $r = 0$ and $n_s = 1 + 2\eta$ where $\eta = -m^2 M_p^2 / V_0$. This model can fit the data very well if $\eta = -0.02$.

3.1.2 Comparison of different pivot scale and the influence of running of spectral index (β_s)

In the former sections, all the fittings are done at pivot scale $k_0 = 0.002 \text{ Mpc}^{-1}$ and the running of spectral index is preferred at more than 2σ level. In this section, we investigate the distributions of α_s at different pivot scales. We use the model $\Lambda\text{CDM}+r+\alpha_s$. The solid line is $k = 0.002 \text{ Mpc}^{-1}$, and the dotted line is $k = 0.025 \text{ Mpc}^{-1}$ in Fig. 7. It shows that when the pivot scale change, the distribution of α_s almost does not change at all. This means that the constraints on α_s is not sensitive to the pivot scale you choose, which indicates that the truncation of power index expansion (Eq. (2.5)) is accurate enough till 1st order.

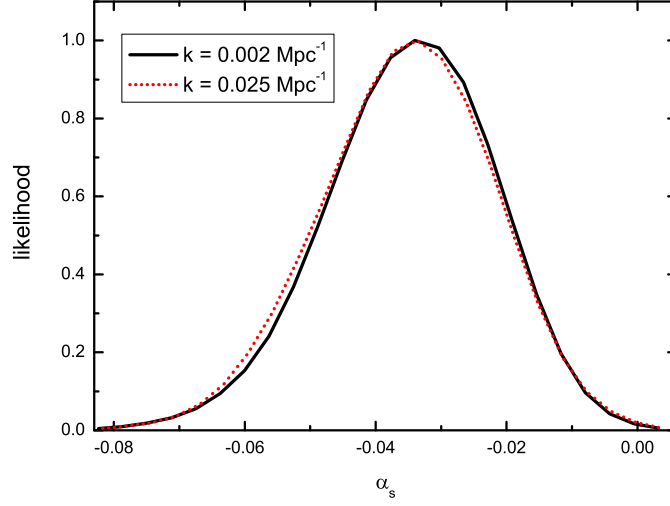


Figure 7: The marginalized distribution of running of spectral index α_s at different pivot scales.

Considering the higher order power effect of the primordial power spectrum, we introduce a new parameter β_s to characterize the “running of running” (Eqs. (2.4) and (2.5)). Left panel of Fig. 8 shows the joint constraint on α_s and β_s , and the right panel shows the marginalized distribution of β_s with a flat prior. We can see that the peak of β_s slightly deviates from 0, but is perfectly consistent with zero within 1σ CL. This means that the current data do not support the “running of running of spectral index”, and therefore the power law expansion of the scalar power spectrum (Eq. (2.5)) is accurate enough till the α_s term. This is consistent with what we find in Sec. 3.1.2. The fitting results are shown in Table 1.

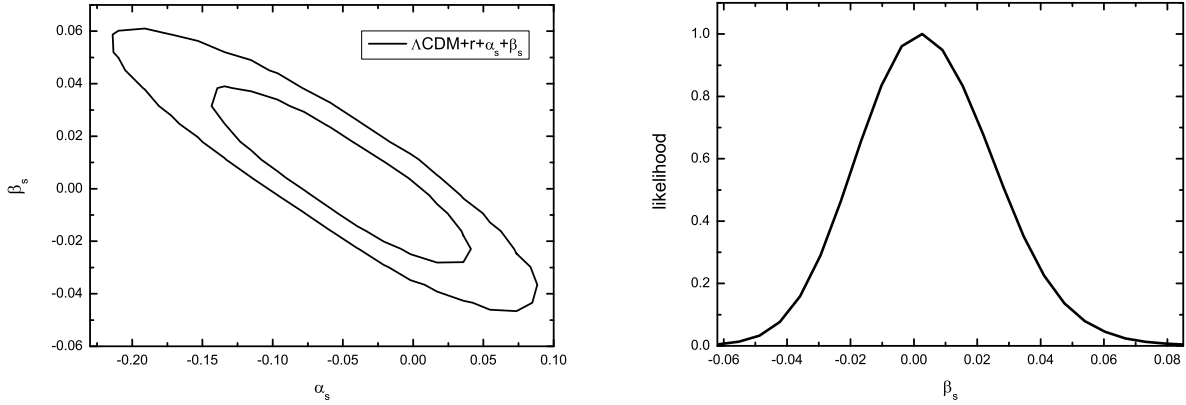


Figure 8: Left: Joint constraints on $\alpha_s - \beta_s$. Right: Marginalized distribution of β_s with 1σ CL 0.005 ± 0.021 .

3.2 General single-field inflation Model (c_s free)

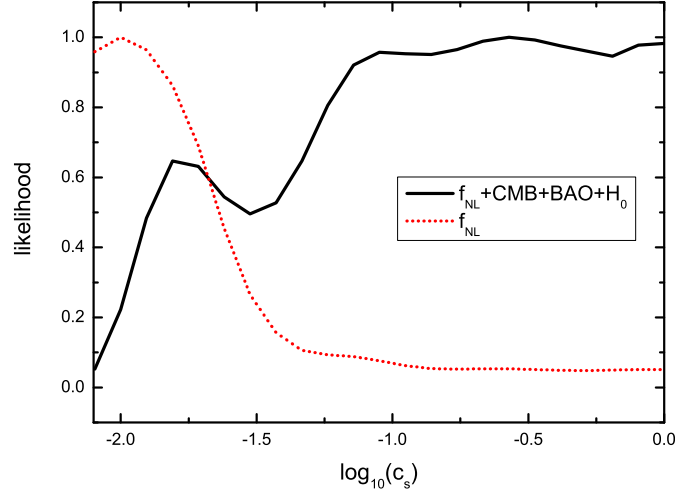


Figure 9: Likelihood of c_s in different datasets.

In this section, we release c_s as a free parameter which is constrained by the f_{NL} data from *WMAP* 9-year results [7]⁴. Table. 2 shows the best fit ($-\log(\text{Like})$) and confidence level of n_s , r and α_s of two models. It can be seen that adding α_s significantly reduces the best fit $-\log(\text{Like})$, but enlarge both the confidence interval of r and n_s .

Fig. 9 shows the distribution of c_s . The dotted line is the likelihood from f_{NL} data while the solid line is marginalized probabilities from the CMB+BAO+ H_0 + f_{NL} data. We can see that the f_{NL} prefers a very low value of c_s while the CMB data sets prefer a larger value, which indicates some tension between each other. In addition, the combined constraints are dominated by CMB power spectrum simply because the number of CMB power spectrum data is far greater than the f_{NL} data. The tension between the f_{NL} data and the CMB power spectrum data may have a variety of indications:

- 1) it may indicate that the power spectrum and bispectrum data are not consistent with each other, which suggests that there are some uncleaned systematics in the data sets;
- 2) it may also indicate that the underlying model, i.e. single-field inflation cannot work at all when we confront it with CMB power spectrum and bispectrum data.

In any case, we need to develop a method which can direct relate c_s with power spectrum and bispectrum (not just f_{NL} data) and globally fit this parameter by using full spectrum of CMB data. Such work is in progress.

4. Conclusion

In this paper, we combine the most recent pre-*Planck* CMB data to constrain the inflation

⁴A similar constraint from *WMAP* 7-year data and Background Imaging of Cosmic Extragalactic Polarization (BICEP) experiment was given in [10].

Table 2: Results of fitting with c_s as a free parameter. Here we use the same k_0 and l_{max} as Table 1.

	$\Lambda\text{CDM}+r$	$\Lambda\text{CDM}+r+c_s$	$\Lambda\text{CDM}+r+c_s+\alpha_s$
n_s	0.959 ± 0.006	0.958 ± 0.006	1.064 ± 0.040
$r(95\%CL)$	< 0.12	< 0.11	< 0.40
α_s	—	—	-0.034 ± 0.012
Best fit $-\ln(\text{Like})$	4921.15	4922.14	4918.17
$\Delta\chi^2$	0	1.98	-5.96

model parameters. Our data consists of *WMAP* 9-year data [4], ACT data [6], SPT data [5], Baryon Acoustic Oscillation data [13] as well as H_0 prior [14]. We mainly find four interesting results from our numerical fitting:

- if we add in the running of spectral index $\alpha_s = dn_s/d\ln k$, the χ^2 value reduces a lot, which indicates that it improves the fit to data very much.
- By adding in a ‘3rd-order’ parameter, i.e. running of running β_s , we find that current data do not support non-zero detection of β_s . In addition, by switching to different pivot scales, the constraints on α_s do not vary a lot. These two tests strongly suggest that the expansion of the power spectrum is accurate enough till the 1st order (α_s term), and there is no observational hint for the higher order scale-dependent terms.
- Due to the new ACT and SPT data we used, our constraints on $r - n_s$ is tighter than the *WMAP* 9-year results [4]. Our constraints is already able to rule out a large class of single-field inflation model even before *Planck* data. We show that the single field inflation with power law ϕ^p can only survive if p is in between 0.9 and 2.1, and Spontaneously broken SUSY (SBS) inflation is ruled out firmly by current observational data.
- We release sound speed c_s as a free parameter, and find that the constraints on c_s from f_{NL} data and CMB power spectrum are not consistent with each other. This strongly indicates that either there is some unaccounted systematics in the bispectrum data that may incur extra-error in the f_{NL} estimation, or the model of varying c_s cannot work at all given these two datasets. In any case, this motivates us to explore a set of formulism that directly compute power spectrum and bispectrum given a c_s value.

In conclusion, we find that pre-*Planck* data have already been able to set tight constraints on single field inflation model. But current observational data still leave many open questions to be solved. We hope such issues will be resolved when the *Planck* data becomes available in a few days.

Acknowledgement— We would like to thank Mark Halpern to share his figure with us. This work is supported by the project of Knowledge Innovation Program of Chinese

Academy of Science and a grant from NSFC (grant NO. 10821504).

References

- [1] A. H. Guth, Phys. Rev. D **23**, 347 (1981)
- [2] A. D. Linde, Phys. Lett. B **108**, 389 (1982)
- [3] A. Albrecht and P. J. Steinhardt, Phys. Rev. Lett. **48**, 1220 (1982).
- [4] G. Hinshaw, D. Larson, E. Komatsu, D. N. Spergel, C. L. Bennett, J. Dunkley, M. R. Nolta and M. Halpern *et al.*, arXiv:1212.5226 [astro-ph.CO].
- [5] K. T. Story, C. L. Reichardt, Z. Hou, R. Keisler, K. A. Aird, B. A. Benson, L. E. Bleem and J. E. Carlstrom *et al.*, arXiv:1210.7231 [astro-ph.CO].
- [6] J. L. Sievers, R. A. Hlozek, M. R. Nolta, V. Acquaviva, G. E. Addison, P. A. R. Ade, P. Aguirre and M. Amiri *et al.*, arXiv:1301.0824 [astro-ph.CO].
- [7] C. L. Bennett, D. Larson, J. L. Weiland, N. Jarosik, G. Hinshaw, N. Odegard, K. M. Smith and R. S. Hill *et al.*, arXiv:1212.5225 [astro-ph.CO].
- [8] J. Garriga and V. F. Mukhanov, Phys. Lett. B **458**, 219 (1999) [hep-th/9904176].
- [9] J. A. Vazquez, M. Bridges, Y. Z. Ma, & M. P. Hobson, 1303.4014 [arXiv:astro-ph.CO]
- [10] C. Cheng, Q. -G. Huang, X. -D. Li and Y. -Z. Ma, Phys. Rev. D **86**, 123512 (2012) [arXiv:1207.6113 [astro-ph.CO]].
- [11] Q. -G. Huang, JCAP **0611**, 004 (2006) [astro-ph/0610389].
- [12] Q. -G. Huang, Phys. Rev. D **76**, 043505 (2007) [astro-ph/0610924].
- [13] Beutler, F., *et al.*, Mon. Not. Roy. Astron. Soc. **416**, 3017 (2011); Padmanabhan, N., Xu, X., Eisenstein, D. J., Scalzo, R., Cuesta, A. J., Mehta, K. T., & Kazin, E. 2012, [astro-ph.CO], arXiv:1202.0090; L. Anderson, E. Aubourg, S. Bailey, D. Bizyaev, M. Blanton, A. S. Bolton, J. Brinkmann and J. R. Brownstein *et al.*, Mon. Not. Roy. Astron. Soc. **428**, 1036 (2013) Blake, C., *et al.*, Mon. Not. Roy. Astron. Soc. **425**, 405 (2012)
- [14] A. G. Riess, *et al.*, ApJ **730**, 119 (2011)
- [15] A. Lewis, Phys. Rev. D **70**, 043011 (2004); A. Lewis, A. Challinor and A. Lasenby, AJ **538**, 473 (2000); <http://www.camb.info>
- [16] A. Lewis and S. Bridle, Phys. Rev. D **66**, 103511 (2002); <http://cosmologist.info/cosmomc/>
- [17] A. Lewis and S. Bridle, Phys. Rev. D, **66**, 103511 (2012)
- [18] A. D. Linde, Phys. Lett. B **129**, 177 (1983).
- [19] L. McAllister, E. Silverstein and A. Westphal, Phys. Rev. D **82**, 046003 (2010) [arXiv:0808.0706 [hep-th]].
- [20] G. R. Dvali, Q. Shafi and R. K. Schaefer, Phys. Rev. Lett. **73**, 1886 (1994) [hep-ph/9406319]; E. J. Copeland, A. R. Liddle, D. H. Lyth, E. D. Stewart and D. Wands, Phys. Rev. D **49**, 6410 (1994); P. Binetruy and G. R. Dvali, Phys. Lett. B **388**, 241 (1996) [hep-ph/9606342]; E. D. Stewart, Phys. Rev. D **51**, 6847 (1995) [hep-ph/9405389]; D. H. Lyth and A. Riotto, Phys. Rept. **314**, 1 (1999) [hep-ph/9807278].
- [21] E. D. Stewart, Phys. Lett. B **391**, 34 (1997) [hep-ph/9606241]; E. D. Stewart, Phys. Rev. D **56**, 2019 (1997) [hep-ph/9703232].